Unravelling Molecular Aspects of the Migratory Insertion Step in Cp*Co^{III} Metallacyclic Systems

Jesús Sanjosé-Orduna,[†,‡] Jordi Benet-Buchholz,[†] Mónica H. Pérez-Temprano*,[†]

† Institute of Chemical Research of Catalonia (ICIQ). The Barcelona Institute of Science and Technology (BIST). Avgda. Països Catalans 16, 43007 Tarragona, Spain

‡ Departament de Química Analítica i Química Orgànica, Universitat Rovira i Virgili, C/ Marcel·li Domingo s/n, 43007 Tarragona, Spain

Supporting Information Placeholder

ABSTRACT: This Forum article describes the reactivity and regioselectivity of the insertion of electrophiles, such as alkynes and alkenes, into Co–C bonds in the context of Cp*Co-catalyzed C–H functionalization reactions. The mechanistic investigation, using diphenylacetylene as model system, reveals that the rate-determining step of the insertion process depends on the temperature. The reaction of a catalytically relevant cobaltacycle, [Cp*Co^{III}(2-ppy)(MeCN)](BF$_4$), with selected terminal electrophiles, such as phenylacetylene, styrene and vinyl acetate, unravel different insertion modes depending on the nature of the unsaturated molecule. The inserted products were fully characterized by NMR spectroscopy, MS-ESI and single crystal X-ray diffraction. In addition, we performed a kinetic study to establish their relative reactivity.

INTRODUCTION

Over the past few years, cobalt catalysts have emerged as a potential alternative to precious metals in directed C–H functionalization reactions.[1] When compared to noble metals, cobalt catalysts offer obvious advantages, including being earth-abundant and cheaper. However, the most interesting feature of cobalt catalysts is the potential rich manifold of reactivity patterns that they can provide, not only mimicking precious metals but also exhibiting a unique and versatile reactivity. This is likely due to its low electronegativity, small radius and facile access to multiple oxidation states through 1 or 2 electron processes. Surprisingly, the first example of chelation-assisted transition-metal catalyzed C–H functionalization was reported by Murahashi, as early as in 1950s, using a cobalt catalyst (Scheme 1).[2] However, it took more than 50 years to rediscover the potential of cobalt-catalyzed directed C–H functionalization in organic synthesis.[1]

Scheme 1. First ligand-assisted transition metal-catalyzed C–H functionalization reaction

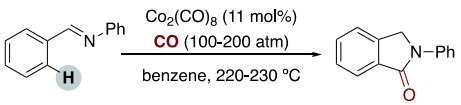

In this context, the employment of Cp*Co^{III} complexes, known since mid-70s,[3] and analogous to active Rh^{III} catalysts for C–H activation,[4] has represented a tremendous advance in cobalt catalysis over the past 5 years.[1,5] Despite the growth of this field, there are relatively few mechanistic insights into these transformations even when using well-established electrophilic coupling partners such as alkenes or alkynes.[1,5,6] One of the main reasons for the lack of fundamental knowledge is the difficulty to detect/characterize/isolate relevant reactive species in these systems.[7] This is likely due to the proposed reversible nature of the C–H metalation step and/or the high reactivity of the transient cobalt intermediates after their reaction with the corresponding coupling partner (Scheme 2).[8] In most cases, the mechanistic knowledge available is limited to H/D exchange experiments, KIE values or the detection of cobalt intermediates by MS-ESI.[1,5,8] These data do not provide structural information, at molecular level, of the cobaltacycle intermediates involved in these transformations.

Scheme 2. Cp*Co-catalyzed directed C–H functionalization reactions

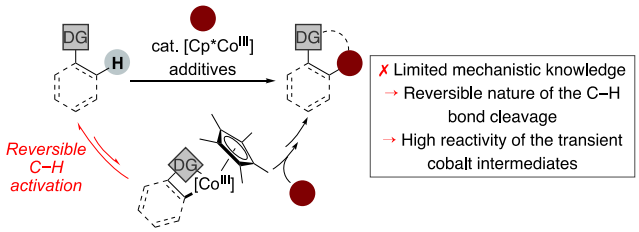

As part of our interest in understanding the reaction mechanisms of Cp*Co^{III}-catalyzed directed C–H functionalization reactions, we recently designed two different synthetic strategies for accessing a direct analogue of one the most widely invoked C–H activated cationic Cp*Co^{III} metallacycles (Scheme 3).[7b,f] Initially, due to the proposed reversibility of the C–H activation step, we explored one of the preferred routes to afford cyclometalated products: oxidative addition reactions.[9] Although the oxidative addition of perfluoroalkyl iodides (R_f–I) to [Cp*Co^{I}(CO)$_2$] to form stable [Cp*Co^{III}(CO)R_fI] complexes is known since the pioneering studies by Stone and King,[10] the preparation of cobaltacycles using this approach was unprecedented at that time. The heteroatom-assisted oxidative addition of 2-(2-iodophenyl)pyridine to [Cp*Co^{I}L$_2$] (L = CO, vinyltrimethylsilane), followed by halide abstraction with $AgBF_4$ in MeCN produced the desired cationic cobaltacycle, **1-MeCN**.[7b] It should worth mentioning that the employment of non-coordinating solvents such as DCM in the salt metathesis led to decomposition. Inspired by these results, we took advantage of the stabilizing capability of MeCN to overcome the reversible nature of the C–H bond cleavage by Cp*Co^{III} and capture otherwise inaccessible cobalt intermediates via C–H activation.[7f] We observed the smooth formation of **1-MeCN** by ^{1}H NMR spectroscopy upon reaction of [Cp*Co^{III}(MeCN)$_3$](BF$_4$)$_2$ with 10 equivalents of 2-ppyH, using the substrate also as a surrogate base.

Scheme 3. Design synthetic routes for accessing 1-MeCN

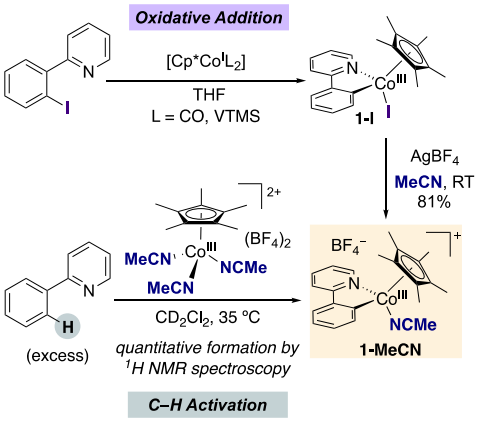

We have used **1-MeCN** to describe, for the first time, a comprehensive mechanistic picture of the most explored reactivity with Cp*Co^{III} catalysts: C–H oxidative alkyne annulations.[7b] Using diphenylacetylene (dpa) as model coupling partner, we were able to detect and characterize in situ the catalyst resting state, a seven-membered ring cobaltacycle (**2a-MeCN**) stabilized by acetonitrile. This highly reactive intermediate was formed by the alkyne coordination and migratory insertion of dpa into the Co–C bond of **1-MeCN**. Stoichiometric reactions of **1-MeCN** with 3 equiv of dpa revealed that the presence of an excess of MeCN slows down not only the formation of **2a-MeCN** but also the reductive elimination step that affords the annulated product. This suggests that the stabilized 18-electron cobaltacycles (**1-MeCN** and **2a-MeCN**) are off-cycle species in equilibrium with the 16-electron complexes (**1** and **2a**) with a vacant coordination site, which are the reactive ones (Scheme 4). Importantly, under stoichiometric conditions, the formation of [Cp*Co^{I}] after the reductive elimination step could be indirectly corroborated by subsequent addition of 2-(2-iodophenyl)pyridine, resulting in the clean formation of **1-I**. Under catalytic conditions, the copper and/or silver salts present in the reaction mixture are presumably responsible for the re-oxidation of the Co^{I} species. The resulting [Cp*Co^{III}] would be the active one in the C–H activation step.[7a,11] (reference)

Scheme 4. Mechanistic investigation on Cp*Co^{III}-catalyzed Oxidative Alkyne Annulation

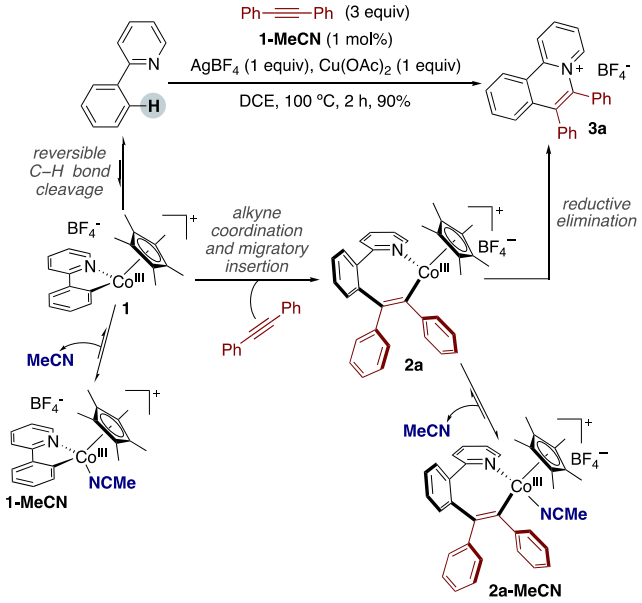

Despite our contributions,[7b,f] and the recent observation of analogous insertion products,[7d-e,g] there are still important fundamental questions regarding the insertion step, fundamental in different Cp*Co-catalyzed C–H functionalization reactions (Scheme 5), that need to be addressed. In sharp contrast to analogous Ir and Rh-based systems,[12] to date, there is a dearth of fundamental information on the reactivity and regioselectivity of the insertion of alkynes or alkenes into Co–C bonds of Cp*Co^{III} cyclometallated complexes.

Scheme 5. Mechanistic proposal of Cp*Co-catalyzed C-H functionalizations involving insertion reactions as key step

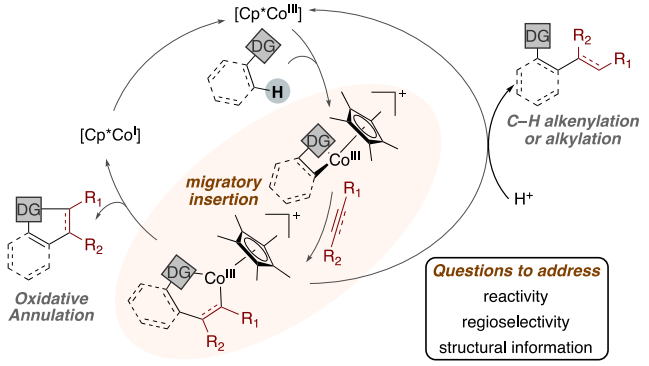

Inspired by our previous results, in this Forum Article, we employ **1-MeCN** as platform to explore previously inaccessible mechanistic intricacies of the migratory insertion step using diphenylacetylene as model system. Our kinetic study reveal that the rate-determining step of the alkyne insertion process can vary depending on the reaction conditions. Moreover, we investigated the reactivity of selected unsaturated molecules with different stereoelectronic properties: diphenylacetylene, phenylacetylene, styrene and vinyl acetate. The molecular structures by X-ray diffraction of the inserted products unravel multiple insertion modes depending on the nature of the unsaturated molecule. The elucidation of this structural information at the molecular level, along with the observed reactivity, is unprecedented in cobalt chemistry.

RESULTS AND DISCUSSION

Mechanistic study on the insertion reaction using diphenylacetylene as model coupling partner.

First, we sought to gain a detailed mechanistic understanding on the insertion of internal alkynes into the cobalt–carbon of Cp*Co^{III} cyclometallated complexes. These electrophiles are the most widely used coupling partner in Cp*Co-catalyzed C–H functionalization reactions.[1,5,6] As shown above, our previous investigation using diphenylacetylene (dpa) as model alkyne system showed that its insertion involves multiple elementary steps when starting from coordinatively saturated cationic cobaltacycles (see Scheme 4).[7b] However, these preliminary studies left several open questions, including the determination of the rate-limiting step of the insertion process or the reactivity of a neutral Cp*Co^{III} cobaltacycles, such as **1-I**, towards dpa.

*1.1 Influence of the Cp*Co^{III} cobaltacycle precursor.* We first investigated the impact of the coordination sphere of the metal center on the outcome of the insertion reaction. It is well-known that the rate of the alkyne insertion is highly dependent on the coordination number of the starting metalacyclic complex.[13] We used our previous results, the reaction of **1-MeCN** with 3 equiv of dpa in DCM-d_2 as benchmark for evaluating these effects in our cobalt system. Under these reaction conditions, we observed the formation of **2a-MeCN** along with the annulated product (**3a**) after 25 minutes at 35 ºC (Figure 1i).

Next, we explored the reactivity of **1-I**. Different literature precedents have shown that neutral cyclometallated complexes [Cp*M (C^N)X] (M = Ir, Rh; C^N = 2-ppy; X = halide) readily undergo alkyne insertion reactions.[12c] Neither traces of a seven-membered ring cobaltacycle or **3a** were detected by ^{1}H NMR spectroscopy upon treatment of **1-I** with 3 equivalents of dpa at 35 ºC for 2 hours in DCM-d_2 (Figure 1i). In sharp contrast, when performing the same reaction, but in the presence of $AgBF_4$ (1.5 equiv), we observed the instantaneous formation of the annulated product (Figure 1iii). Under these reaction conditions, in the absence of a stabilizing ligand such as MeCN, **2a** cannot be observed directly due to its highly reactive nature. This reactivity trend clearly indicates that a facile access to a cationic 16-electron intermediate with a vacant coordination site accelerates the rate of insertion and the reductive elimination process.

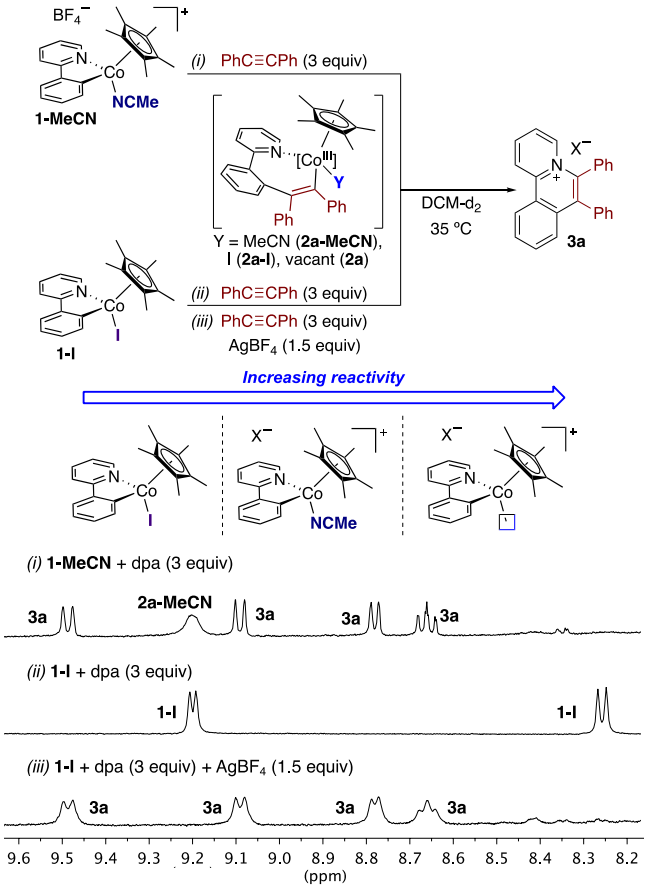

Figure 1. Comparative study on the reactivity of **1-MeCN** and **1-I** towards diphenylacetylene. Reaction conditions: 0.01 mmol of **1-MeCN** or **1-I**, 0.03 mmol of dpa in 0.5 mL of CD_2Cl_2, 35 ºC, 25 min. For (iii), 0.015 mmol of $AgBF_4$ was added.

1.2 MeCN effect. We next determined the order of the alkyne insertion reaction respect to MeCN using **1-MeCN**. Since the reductive elimination product, **3a**, exhibits solubility issues in dichloromethane, the initial rates method was used to determine the insertion rate at each [MeCN] in DCM-d_2 at 25 ºC. The experimental data

employed to determine r_0 were obtained within reaction times in which the amount of **3a** did not affect the concentration of the complexes under study. Under these conditions, the concentration of **1-MeCN** and **2a-MeCN**, were monitored by ^{1}H NMR spectroscopy. As expected, increasing amounts of MeCN dramatically slowed the reaction rate.[14] The plot of initial reaction rate (r_0) versus [MeCN]$^{-1}$ was linear, indicating an inverse order on MeCN (Figure 2). This result confirms that the dissociation of MeCN is crucial for generating the reactive unsaturated cobalt species involved in the alkyne insertion process.

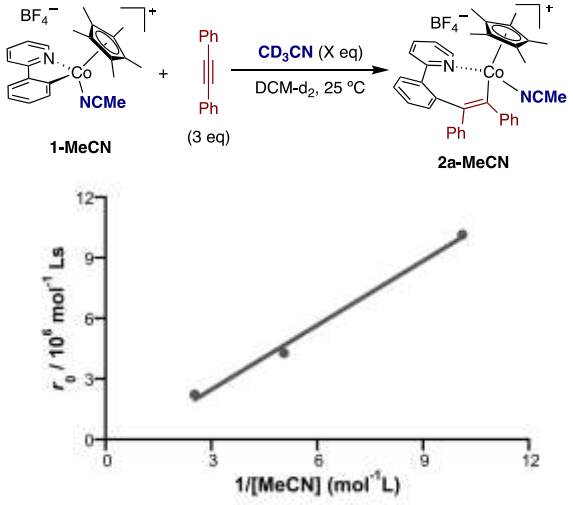

Figure 2. Plot of initial rates versus [MeCN]$^{-1}$ showing inverse order kinetics in acetonitrile. Reaction conditions: 0.01 mmol of **1-MeCN**, 0.03 mmol of dpa in 0.5 mL of CD_2Cl_2, 25 °C. 2.5, 5 and 10 μL CD_3CN were added, respectively.

1.3 Influence of the diphenylacetylene. We next investigated the dependence of the reaction rate of the alkyne insertion on the concentration of diphenylacetylene (dpa). We monitored the reaction between **1-MeCN** and different amounts of added dpa (3 or 10 equiv), in the presence of 5 equiv of MeCN, in DCM-d_2 at 35 °C.[15] Despite the solubility problems associated to the formation of **3a** under these reactions conditions, which hamper the NMR monitoring,[16] we observed that the reaction rate clearly depends on the concentration of dpa as shown in Figure 3, accelerating the formation of **2a-MeCN**.

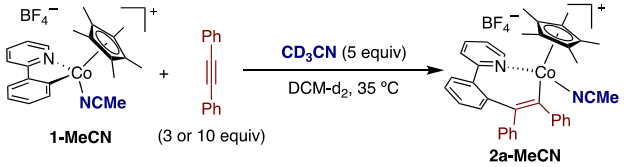

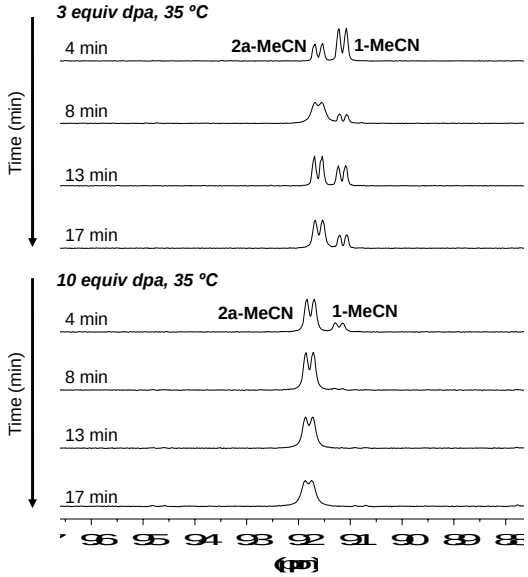

Figure 3. Influence of dpa on the alkyne insertion process at 35 °C. Reaction conditions: 0.01 mmol of **1-MeCN**, 0.03 or 0.1 mmol of dpa in 0.5 mL of CD_2Cl_2, 35 °C.

Next, we carried out these reactions at lower temperature, 0 °C, in the absence of added MeCN. Under these reaction conditions, the product formation is sufficiently slow to allow the study of the alkyne insertion step independently. Surprisingly, the formation of **2a-MeCN** is zero-order dependence on [dpa] (Figure 4). Similar values of r_0 were found for $[dpa]_0 = 0.06$ or 0.2 mol L^{-1} resulting $r_0 = 2.7\times10^6$ mol L^{-1} s^{-1} and $r_0 = 3.0\times10^6$ mol L^{-1} s^{-1}, respectively.

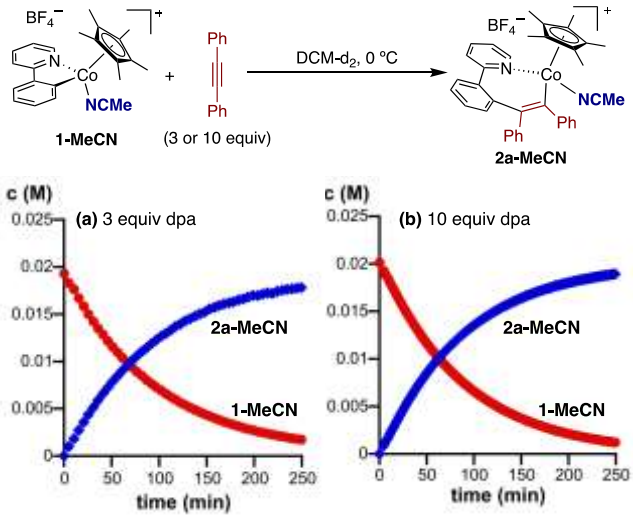

Figure 4. Alkyne insertion process at 0°C in the presence of different amounts of dpa. Reaction conditions: 0.01 mmol of **1-MeCN**, 0.03 or 0.1 mmol of dpa in 0.5 mL of CD_2Cl_2, 0 °C.

Although the reaction conditions are slightly different at 0 °C and 35 °C, the effect of [dpa] on the alkyne reaction rate suggests a temperature-dependent change in the rate-determining step in the alkyne insertion process. At 35 °C,

the insertion of the alkyne into the Co–C bond is presumably the rate-determining step while at 0 ºC, the alkyne seems not to be involved.

1.4 Eyring plot. In order to gain further insights into the rate-determining step of the alkyne insertion process at low temperature, we calculated the activation parameters. We monitored the reaction of **1-MeCN** with 3 equiv of dpa in the temperature range from –10 to 10 ºC by ^{1}H NMR spectroscopy. The rate constants (k_1) were obtained by fitting the concentration versus time data to the kinetic model shown in Figure 5, by nonlinear least-squares (NLLS) regression,[17] considering that the reaction is zero-order with respect to dpa. This figure shows the data at -10 ºC as a representative example.

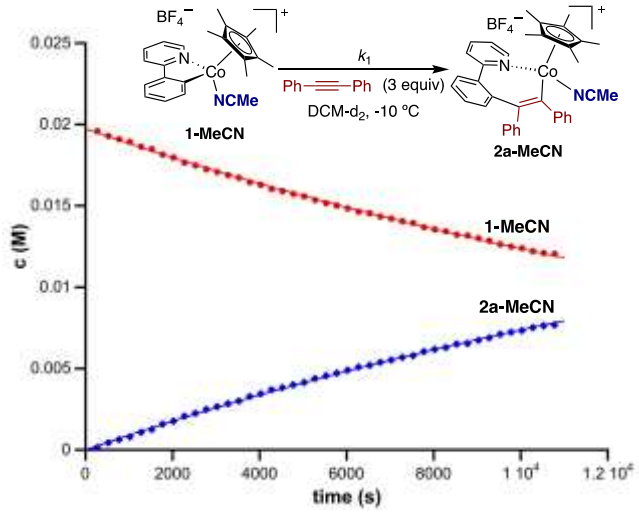

Figure 5. Alkyne insertion process at -10ºC. Solid lines are the best fit using GEPASI. Reaction conditions: 0.01 mmol of **1-MeCN**, 0.03 mmol of dpa in 0.5 mL of CD_2Cl_2, –10 ºC.

The activation parameters were determined using the Eyring equation, affording the following values: $\Delta H^{\ddagger}$ = 21.0 ± 1.95 kcal mol^{-1}; $\Delta S^{\ddagger}$ = 1.61 ± 0.24 cal K^{-1} mol^{-1} (Figure 6). Although, the calculated $\Delta S^{\ddagger}$ is not large, its positive value, along with the zero-order dependence on alkyne suggest, that at low temperature, the dissociation of MeCN, prior to the migratory insertion, could be the rate-determining step.

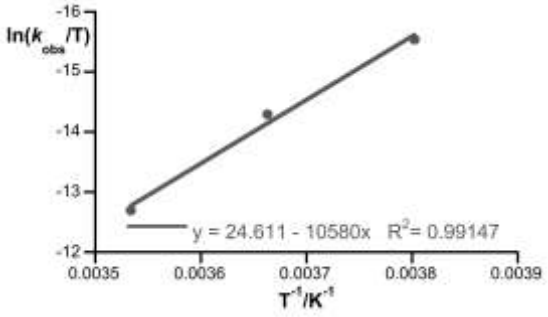

Figure 6. Eyring plot for determination of $\Delta H^{\ddagger}$ and $\Delta S^{\ddagger}$ for the alkyne insertion at low temperature.

Reactions of 1-MeCN with terminal unsaturated electrophiles. Next, we aimed to unravel the reactivity and insertion modes of selected unsaturated model molecules such as phenylacetylene, styrene and vinylacetate. For diphenylacetylene, we have reported the formation of a seven-membered cobaltalcycle, **2a-MeCN**, through the traditional 1,2-insertion mode. However, other type of products could be potentially formed whether the corresponding electrophile inserts into the Co–C bond multiple times or if the insertion occurs in a 1,1-fashion (Figure 7). We have targeted these terminal alkynes and alkenes for our reactivity study since different literature reports have shown these non-traditional insertion modes with analogous Cp*Ir^{III}- and Cp*Rh^{III}-based systems.[12]

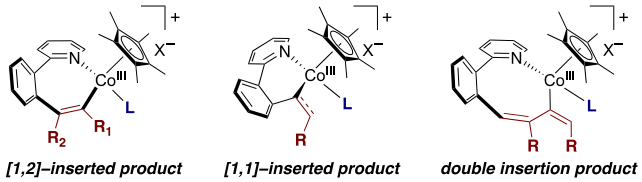

Figure 7. Potential insertion modes

Based on our previous knowledge, we attempted to access the inserted products following an analogous procedure than the previously described for dpa, using **1-MeCN** as the starting complex (Scheme 6). As for **2a-MeCN**, the corresponding inserted products when using phenylacetylene and styrene were not isolable. However, inspired by our mechanistic insights, we added a high excess of MeCN to enable the full characterization of **2b-MeCN** and **2c-MeCN** by NMR spectroscopy (1D and 2D experiments), and MS-ESI.[18] In sharp contrast, **2d** exhibits high stability and it was isolated in a quantitative manner. In all cases, we observed a single inserted product. Phenylacetylene and vinyl acetate insert into the Co–C bond of **1-MeCN** in a completely regiospecific 1,2-manner. For analogous rhodium systems, Jones and co-workers have reported the formation of doubled-insertion products when using phenylacetylene as electrophile.[12c] In our case, we did not observe the formation of these type of products. A rhodacycle analogous to **2d** has been described by Ellman and co-workers as a catalyst resting state of the Cp*Rh^{III}-catalyzed directed C–H vinylation using vinyl acetate as a vinyl source.[19] Surprisingly, the [1,1]-insertion product is obtained when using styrene. The observation and characterization of **2c-MeCN** is particularly relevant since, to date, the formation of this type of inserted product had not been proposed in Cp*Co-catalyzed C–H functionalization products.[11a,20] The preference for six-membered-ring metallacycles over seven-membered ones when using alkenes as coupling partners have been reported for Cp*Rh^{III} cyclometalated complexes.[12c]

Scheme 6. Reactivity of 1-MeCN with terminal electrophiles

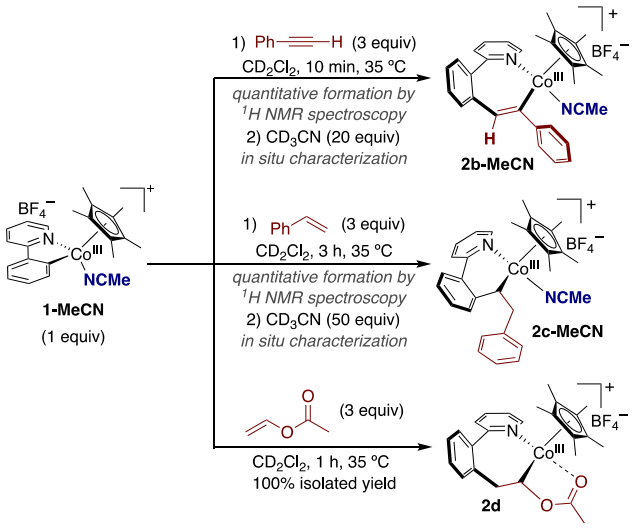

The structural and spectroscopic characterization of these cobalt complexes displayed interesting features at molecular level. As observed for **2a-MeCN**, the ^{1}H NMR spectra of the inserted products show an upfield displacement of the chemical shift of the Cp* ligand compared to **1-MeCN**. This can be explained due to the anisotropic action of a ring current of the cyclometalated phenyl. When using the terminal alkenes, the coupling patterns of the resulting alkylic protons are analogous. In both cases, we observed three different signals, since the protons of the methylene group are diastereotopic. However, the chemical shift of the alkylic CH varies dramatically, 4.73 ppm and 7.86 ppm for **2c-MeCN** and **2d**, respectively.

Table 1. Selected bonds and angles for the single crystal structures measured.

Distance [Å] / angle [°]	1-MeCN[1]	2a-MeCN[1]	2b-MeCN	2c-MeCN	2d
Co-N_{ppy}	1.959(3)	2.011(2)	1.9822(10)	1.980(8)	1.991(3)
Co-N_{ACN}	1.905(4)	1.928(3)	1.9242(11)	1.917(11)	---
Co-C_A[2]	1.936(4)	1.984(3)	1.9775(12)	2.051(7)	1.960(3)
N_{ppy}-Co-N_{ACN}[3]	91.46(13)	89.47(10)	91.85(4)	92.2(6)	90.61(11)
N_{ppy}-Co-C_A	82.39(15)	90.49(10)	90.60(4)	86.93(9)	97.13(14)
Co-N_{ACN}-C_{1ACN}	173.6(3)	175.7(2)	170.55(10)	166.38(9)	---
Torsion 1[4]	0.6(5)	61.2(4)	55.18(17)	33.9(13)	45.6(5)

1: From Ref 7b. 2: C_A is the carbon atom attached to the Cobalt. 3: In 2d it corresponds to the angle between N_{ppy}, Cobalt and the O corresponding to the acetate. 4: Torsion angle at 2ppy.

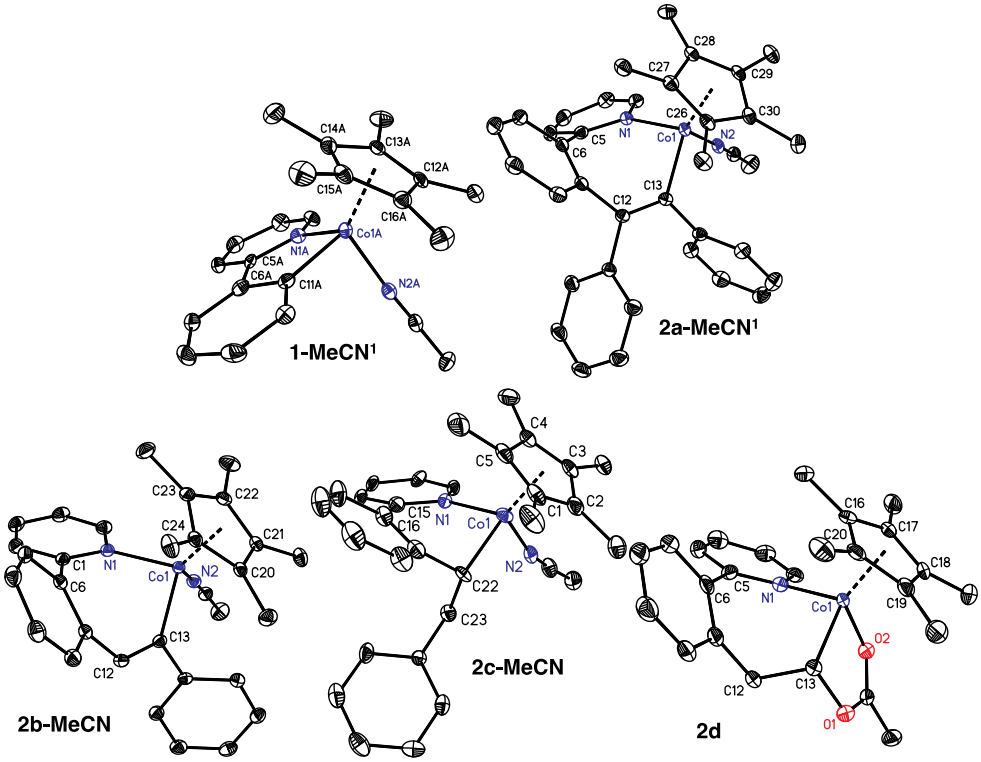

Figure 8. ORTEP-plots of **2a-MeCN**, **2b-MeCN**, **2c-MeCN**, **2d**, respectively. Thermal ellipsoids drawn at 50% probability, hydrogen atoms, BF_4 anions and additional molecules in the unit cell were omitted for clarity.

The structures of the inserted products were unequivocally confirmed by single-crystal X-ray diffraction (see Table 1, Figure 8). As **1-MeCN** and **2a-MeCN**, all three structures show a three-legged piano stool geometry. For **2b-MeCN**, the phenyl group of the PhC≡CH is preferentially located adjacent to the metal center after the alkyne insertion, indicating the dominance of the electronic effects. The solid-state structures of **2c-MeCN** and **2d** show that a subtle modification on the nature of the terminal alkenes can induce different insertion modes. While styrene affords a six-membered ring cobaltacycle via a [1,1]-insertion, vinyl acetate undergoes a traditional [1,2]-mode. In this case, the acetate is coordinated to the cobalt metal center instead of a molecule of acetonitrile.

The C_A–Co–N_{ppy} bite angle of the inserted products are larger than the one for **1-MeCN** [82.39(15)º]. The phenyl rings are rotated out of the plane of the pyridine with a dihedral angle, ranging from 33.9(13) for **2c-MeCN** to 61.2(4)º for **2a-MeCN**, which are much larger than the one observed for **1-MeCN** (0.6(5)º). It should be worth mentioning that the Co–N_{ppy}, Co–N_{ACN} and Co–C_A bond lengths for the inserted products are longer than for **1-MeCN**.

2.1 Reactivity of terminal versus internal alkyne. With this structural information in hand, we compared the behavior of terminal and internal alkynes. We monitored the reaction of **1-MeCN** with 3 equiv of alkyne, PhC≡CPh or PhC≡CH, in DCM-d_2 at 35 ºC, in the presence of 5 equiv of MeCN, in order to stablish their relative reactivity. We selected these reaction conditions, where the formation of the annulation product is very slow, to simplify the systematic study by ^{1}H NMR spectroscopy. Comparing the kinetic experiments with PhC≡CPh and PhC≡CH, it is found that PhC≡CH reacts faster than the internal alkyne (Figure 9). Although we did not quantify the formation of the reductive elimination products, since they exhibit low solubility in DCM, we detected the formation of **3a** at longer reaction times, while the seven-membered ring cobaltacycle **2b-MeCN** does not undergo reductive elimination under our reaction conditions. These results suggest that the alkyne insertion is favored for phenylacetylene while the reductive elimination process is facilitated when using dpa.

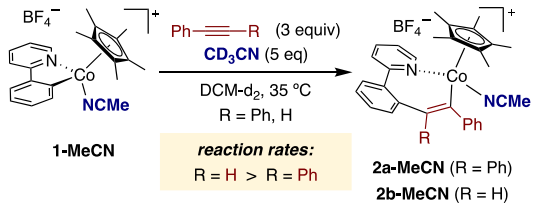

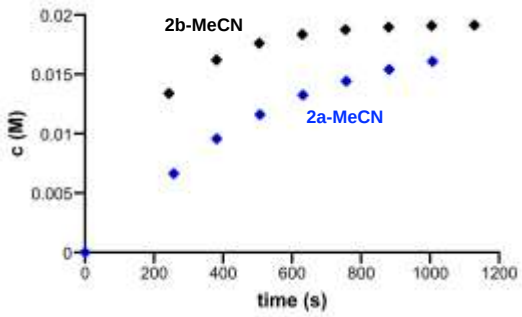

Figure 9. Reactivity of terminal versus internal alkynes. Reaction conditions: 0.01 mmol of **1-MeCN**, 0.03 of dpa or phenylacetylene, 0.05 mmol of CD_3CN in 0.5 mL of CD_2Cl_2, 35 ºC.

2.2 Reactivity of phenylacetylene versus styrene. We monitored the reaction of **1-MeCN** with 3 equiv of styrene in DCM-d_2 at 35 ºC, in the presence of 5 equiv of MeCN, in order to establish its relative reactivity towards phenylacetylene, the analogous terminal alkyne. Under these reaction conditions, we observed a dramatic difference in the insertion rate. While **2b-MeCN** is formed quantitatively after 20 minutes, we only observed traces of the corresponding inserted product with styrene (Figure 10). These experimental results could be explained taking into account the nature of the electrophile and the resulting inserted product. It is well-known that alkene insertions into M–C bonds are thermodynamically disfavored compared to alkyne ones due to the challenging C–C π-bond cleavage of the olefin. Moreover, the strength of the new M–C_{sp2} bond on the alkyne insertion product is higher than the M–C_{sp3} bond for olefins.[13]

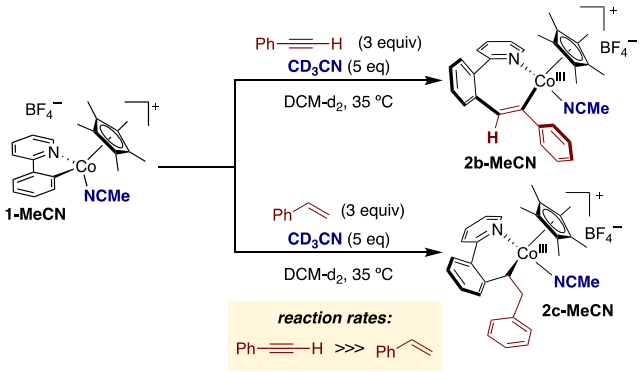

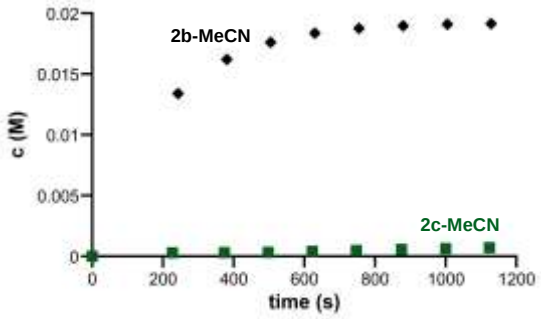

Figure 10. Reactivity of phenylacetylene versus styrene. Reaction conditions: 0.01 mmol of **1-MeCN**, 0.03 of dpa or styrene, 0.05 mmol of CD_3CN in 0.5 mL of CD_2Cl_2, 35 ºC.

2.3 Reactivity of styrene versus vinyl acetate. Finally, we determined the relative reactivity between the two targeted terminal alkenes. As shown in Figure 11, the insertion of styrene to afford **2c-MeCN** occurs at extreme slowness compared to vinyl acetate. Under analogous reactions conditions, we observed almost quantitative formation of **2d** after 50 minutes, while at that time less than 10% of the six-membered ring cobaltacycle is detected by ^{1}H NMR spectroscopy. A plausible hypothesis which explains these experimental data is that the acetate might facilitate an assisted-alkene insertion acting as a chelating ligand. In alignment with this assumption, when we tried the insertion reaction with vinyl ethyl ether, we did not observe the inserted product, even in the absence of added CD_3CN.

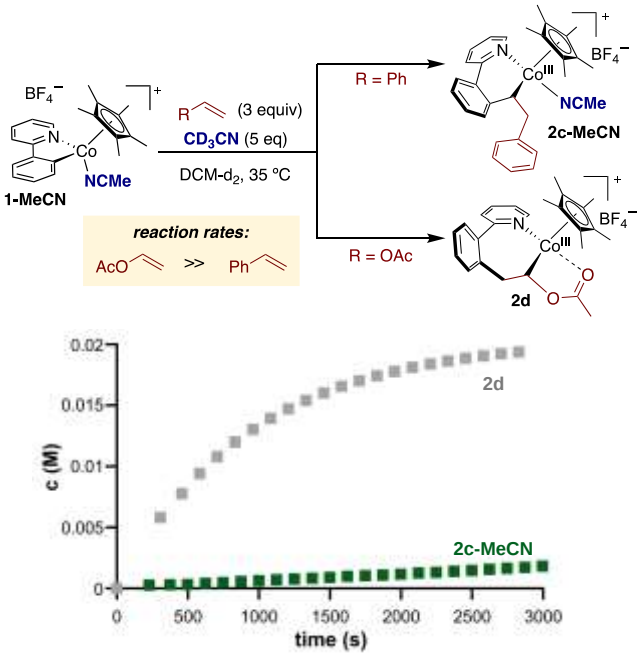

Figure 11. Reactivity of styrene versus vinyl acetate. Reaction conditions: 0.01 mmol of **1-MeCN**, 0.03 of styrene or vinyl acetate, 0.05 mmol of CD_3CN in 0.5 mL of CD_2Cl_2, 35 ºC.

CONCLUDING REMARKS

In conclusion, this work explores one of the fundamental steps in Cp*Co-catalyzed C–H functionalization reactions: the migratory insertion. We have used a direct analogue of a C–H activated Co^{III} metallacycle, [Cp*Co^{III}(2-ppy)(MeCN)](BF$_4$] (**1-MeCN**), for providing previously inaccessible mechanistic intricacies on the reactivity and regioselectivity of the insertion of selected alkynes and alkenes into the Co–C bond. Our initial mechanistic study, using diphenylacetylene as model electrophile, revealed a temperature-dependence of the rate-determining step (rds). At 35 ºC, the insertion of the alkyne into the Co–C bond seems to be the rds. In sharp contrast, at low temperature, 0 ºC, the insertion reaction is zero-order in electrophile, suggesting that the dissociation of MeCN from **1-MeCN**, to generate a reactive 16-electron complex, it is the rate-determining step.

The reaction of our cobalt platform with terminal electrophiles unraveled different insertion modes depending on the nature of the unsaturated molecule. The reactions with phenylacetylene and vinyl acetate afford the expected seven-membered ring cobaltacycles via a traditional [1,2]-insertion. However, the treatment of **1-MeCN** with styrene provides a six-membered ring complex, presumably due to a [1,1]-insertion. The inserted products were fully characterized by NMR spectroscopy, ESI-MS and single crystal X-ray diffraction. The reactivity comparison between the tested electrophiles shows that phenylacetylene provides the fastest alkyne insertion while styrene provides the slowest one.

The results provided herein not only reveal mechanistic information on the migratory insertion process in the context of Cp*Co-catalyzed C–H functionalization reactions but also demonstrate that subtle modifications of the structure of the employed electrophile can produce a significant change on the nature of the transient cobalt species at a molecular level.

ASSOCIATED CONTENT

Supporting Information.
The Supporting Information is available free of charge on the ACS Publications website.
Complete experimental details, including general considerations, kinetic studies and the full characterization of the new compounds, including NMR spectra and X-ray diffraction analysis. (PDF)

Accession Codes
CCDC 1909807 (**2c-MeCN**), 1909808 (**2b-MeCN**) and 1909809 (**2d**) contain the supplementary crystallographic data for this paper. These data can be obtained free of charge via www.ccde.cam.ac.uk/data_request/cif.

AUTHOR INFORMATION

Corresponding Author

*E-mail: mperez@iciq.es

ORCID

Mónica H. Pérez-Temprano: 0000-0003-4818-7990

Jesús Sanjosé-Orduna: 0000-0002-9942-502X

Author Contributions

The manuscript was written through contributions of all authors. All authors have given approval to the final version of the manuscript.

Notes

The authors declare no competing financial interest.

ACKNOWLEDGMENT

We thank the CERCA Programme/Generalitat de Catalunya and the Spanish Ministry of Economy, Industry and Competitiveness (MINECO: CTQ2016-79942-P, AIE/FEDER, EU) for the financial support. J. S.-O. thanks Severo Ochoa Excellence Accreditation for a pre-doctoral contract. We thank the NMR and High Resolution Mass Spectrometry units at the Institute of Chemical Research of Catalonia (ICIQ).

REFERENCES

(1) For selected recent reviews on cobalt-catalyzed directed C–H functionalization reactions, see: (a) Gao, K.; Yoshikai, N. Low-valent cobalt catalysis: New opportunities for C–H functionalizations. *Acc. Chem. Res.* **2014**, *47*, 1208–1219. (b) Tilly, D.; Dayaker, G.; Bachu, P. Cobalt mediated C–H bond functionalization: emerging tools for organic synthesis. *Catal. Sci. Technol.* **2014**, *4*, 2756–2777. (c) Ackermann, L. Cobalt-catalyzed C–H arylations, benzylations, and alkylations with organic electrophiles and beyond. *J. Org. Chem.* **2014**, *79*, 8948–8954. (d) Su, B.; Cao, Z.-C.; Shi, Z.-J. Exploration of earth-abundant transition metals (Fe, Co, and Ni) as catalysts in unreactive chemical bond activations. *Acc. Chem. Res.* **2015**, *48*, 886–896. (e) Moselage, M.; Ackermann, L. Cobalt-catalyzed C–H activation. *ACS Catal.* **2016**, *6*, 498–525. (f) Pototschnig, G.; Maulide, N.; Schnürch, M. Direct Functionalization of C–H bonds by Iron, Nickel, and Cobalt catalysis. *Chem. Eur. J.* **2017**, *23*, 9206–9232. (g) Gandeepan, P.; Müller T.; Zell, D.; Cera, G.; Warrantz, S.; Ackermann, A. 3d transition metals for C–H activation. *Chem. Rev.* **2019**, *119*, 2192–2452.

(2) Murahashi, S. Synthesis of phthalimidines from Schiff bases and carbon monoxide. *J. Am. Chem. Soc.* **1995**, *77*, 6403–6404.

(3) (a) King, R. B.; Efraty, A.; Douglas, W. M. Pentamethylcyclopentadienlyl Derivatives of Transition Metals. III. Some Reactions of Pentamethylcyclopentadienyl-metal Carbonyl Derivatives of Cobalt and Manganese. *J. Organomet. Chem.*, **1973**, *56*, 345–355. (b) Fairhurst, G.; White, C. Syntheses of Pentamethylcyclopentadienylcobalt(III) Compounds and Reactions of $[Co(C_5Me_5)(solvent)_3]X_2$ (solvent = acetonitrile or acetone, X = BF_4 or PF_6). *J. C. S. Dalton*, **1979**, 1524–1530. (c) Fairhurst, G.; White, C. Cyclopentadienyl- or Pentamethylcyclopentadienyl-(arene)cobalt(III) Complexes: arene = indole, benzene, mesitylene, hexamethylbenzene, 1,4-dihydroxy- and 1-hydroxy-4-methoxytetramethylbenzene *J. C. S. Dalton*, **1979**, 1531–1538. (d) Loginov, D. A.; Shul'pina, L. S.; Muratov, D. V.; Shul'pin. G. B. Cyclopentadienyl cobalt(III) complexes: Synthetic and catalytic chemistry. *Coord. Chem. Rev.* **2019**, *387*, 1–31.

(4) For selected reviews, see: (a) Satoh, T.; Miura, M. Oxidative coupling of aromatic substrates with alkynes and alkenes under rhodium catalysis. *Chem. Eur. J.* **2010**, *16*, 11212−11222. (b) Song, G.; Wang, F.; Li, X. C−C, C−O and C−N bond formation via rhodium(III)-catalyzed oxidative C−H activation. *Chem. Soc. Rev.* **2012**, *41*, 3651−3678. (c) Colby, D. A.; Tsai, A. S.; Bergman, R. G.; Ellman, J. Rhodium catalyzed chelation-assisted C−H bond functionalization reactions. *Acc. Chem. Res.* **2012**, *45*, 814–825. (d) Patureau, F. W.; Wencel-Delord, J.; Glorius, F. Cp*Rh-catalyzed C−H activations. Versatile dehydrogenative cross-couplings of Csp2 C−H positions with olefins, alkynes, and arenes. *Aldrichimica Acta* **2012**, *45*, 31−41. (e) Kuhl, N.; Schröder, N.; Glorius, F. Formal SN-type reactions in rhodium(III)-catalyzed C−H bond activation. *Adv. Synth. Catal.* **2014**, *356*, 1443−1460. (f) Song, G.; Li, X. Substrate activation strategies in rhodium(III)-catalyzed selective functionalization of arenes. *Acc. Chem. Res.* **2015**, *48*, 1007–1020. (g) Shin, K.; Kim, H.; Chang, S. Transtion-metal-catalyzed C−N bond forming reactions using organic azides as the nitrogen source: a journey for the mild and versatile C−H amination.

(5) For selected recent reviews on Cp*Co-catalyzed C−H directed functionalization reactions, see: (a) Wei, D.; Zhu, X.; Niu, J.-L.; Song, M.-P. *ChemCatChem* **2016**, *8*, 1242−1263. (b) Yoshino, T.; Matsunaga, S. (Pentamethylcyclopentadienyl)cobalt(III)-catalyzed C−H bond functionalization: from discovery to unique reactivity and selectivity. *Adv. Synth. Catal.* **2017**, *359*, 1245−1262. (c) Wang, S.; Cheng, S.-Y.; Yu, X.-Q. C−H functionalizations by high-valent Cp*Co(III) catalysis. *Chem. Commun.* **2017**, *53*, 3165−3180. (d) Chirila, P. G.; Whiteoak, C. J. *Dalton. Trans.* **2017**, *46*, 9721−9739. (e) Ghorai, J.; Anbarasan, P. Developments in Cp^*Co^{III}-catalyzed C−H bond functionalizations. *Asian. J. Org. Chem.* **2019**, *8*, 430−455.

(6) (a) Prakash, S.; Kuppusamy, R.; Cheng, C.-H. Cobalt-catalyzed annulation reactions via C−H activation. *ChemCatChem* **2018**, *10*, 683−705. (b) Santhoshkumar, R.; Cheng, C.-H. Hydroarylaitons by cobalt-catalyzed C−H activation. *Beilstein J. Org. Chem.* **2018**, *14*, 2266−2288. (c) Peneau, A.; Guillou, C.; Chabaud, L. Recent advances in $[Cp^*M^{III}]$ (M = Co, Rh, Ir)-catalyzed intramolecular annulation through C−H activation. *Eur. J. Org. Chem.* **2018**, 5777−5794. (d) Ujwaldev, S. M. Harry, N. A.; Divakar, M. A.; Anikumar, G. Cobalt-catalyzed C−H activation: recent progress in heterocyclic chemistry. *Catal. Sci. Technol.* **2018**, *8*, 5983−6018.

(7) (a) Ikemoto, H.; Yoshino, T.; Sakata, K.; Matsunaga, S.; Kanai, M. Pyrroloindolone synthesis via a Cp^*Co^{III}-catalyzed redox-neutral directed C–H alkenylation/annulation sequence. *J. Am. Chem. Soc.* **2014**, *136*, 5424−5431. (b) Sanjosé-Orduna, J.; Gallego, D.; Garcia-Roca, A.; Martin, E.; Benet-Buchholz, J.; Pérez-Temprano, M. H. Capturing elusive cobaltacycle intermediates: a real-time snapshot of the Cp^*Co^{III}-catalyzed oxidative alkyne annulation. *Angew. Chem. Int. Ed.* **2017**, *56*, 12137–12141. (c) Sen, M.; Dahiya, P.; Premkumar, J. R.; Sundararaju, B. Dehydrative Cp*Co(III)-catalyzed C–H bond allenylation. *Org. Lett.* **2017**, *19*, 3699–3702. (d) Yu, X.; Chen, K.; Guo, S.; Shi, P.; Song, C.; Zhu, J. Direct access to cobaltacycles via C–H activation: N-chloroamide-enable room-temperature synthesis of heterocycles. *Org. Lett.* **2017**, *19*, 5348–5351. (e) Sen, M.; Rajesh, N.; Emayavaramban, B.; Premkumar, J. R.; Sundararaju, B. Isolation of Cp*Co(III)-alkenyl intermediate in efficient cobalt catalyzed C–H bond alkenylation with alkynes. *Chem. Eur. J.* **2018**, *24*, 342–346. (f) Sanjosé-Orduna, J.; Sarria Toro, J. M.; Pérez-Temprano, M. H. HFIP-assisted C–H functionalization by Cp^*Co^{III}: access to key reactive cobaltacycles and implication in catalysis. *Angew. Chem. Int. Ed.* **2018**, *57*, 11369–11373. (g) Boerth, J. A.; Maity, S.; Williams, S. K.; Mercado, B. Q.; Ellman, J. A. Selective and synergistic cobalt(III)-catalysed three-component C–H bond addition to dienes and aldehydes. *Nat. Catal.* **2018**, *1*, 673–679.

(8) (a) Gallego, D.; Baquero, E. A. Recent advances on mechanistic studies on C−H activation catalyzed by base metals. *Open. Chem.* **2018**, *16*, 1001−1058. (b) Planas, O.; Chirila, P. G.; Whiteoak, C. J.; Ribas, X. Current mechanistic understanding of cobalt-catalyzed C−H functionalization. *Adv. Organomet. Chem.* **2018**, *69*, 209–282.

(9) Albrecht, M. Cyclometalation using d-block transition metals: fundamental aspects and recent trends. *Chem. Rev.* **2010**, *110*, 576−623.

(10) King, R. B.; Treichel, P. M.; Stone, F. G. A. Chemistry of the Metal Carbonyls. XII. New Complexes Derived from Cyclopentadienylcobalt Dicarbonyl. *J. Am. Chem. Soc.* **1961**, *83*, 3593−3597.

(11) Under catalytic conditions, the presence of acetate in the reaction mixture presumably facilitates the C–H metalation step. See: (a) Zell, D.; Bursch, M.; Müller, V.; Grimme, S.; Ackermann, L. Full selectivity control in cobalt(III)-catalyzed C−H alkylations by switching of the C−H activation mechanism. *Angew. Chem. Int. Ed.* **2017**, *56*, 10378–10382. (b) Qu, S.; Cramer, C. J. Mechanistic study of Cp^*Co^{III}/Rh^{III}-catalyzed directed C−H functionalization with diazo compounds. *J. Org. Chem.* **2017**, *82*, 1195–1204. (c) Wang, W.; Huang, F.; Jiang, L.; Zhang, C.; Sun, C.; Liu, J.; Chen, D. Comprehen-

sive Mechanistic Insight into cooperative Lewis acid/Cp*Co^{III}-catalyzed C−H/N−H activation for the synthesis of isoquinolin-3-ones. *Inorg. Chem.* **2018**, *57*, 2804–2814. (d) Lorion, M. M.; Kaplaneris, N.; Son, J.; Kuniyil, R.; Ackermann, L. Late-stage peptide diversification through cobalt-catalyzed C–H activation: sequential multicatalysis for stapled peptides. *Angew. Chem. Int. Ed.* **2019**, *58*, 1684–1688.

(12) (a) Li, L.; Brennessel, W. W.; Jones, W. D. An efficient low-temperature route to polycyclic isoquinoline salt synthesis via C−H activation with $[Cp^*MCl_2]_2$ (M = Rh, Ir). *J. Am. Chem. Soc.* **2008**, *130*, 12414−12419. (b) Davies, D. L.; Al-Duaij, O.; Fawcett, J.; Singh, K. Reactions of cyclometalated oxazoline half-sandwich complexes of iridium and ruthenium with alkynes and CO. *Organometallics* **2010**, *29*, 1413−1420. (c) Li, L.; Jiao, Y.; Brennessel, W. W.; Jones, W. D. Reactivity and regioselectivity of insertion of unsaturated molecules into M−C (M = Ir, Rh) bonds of cyclometalated complexes. *Organometallics* **2010**, *29*, 4593−4605. (d) Boutadla, Y.; Davies, D. L.; Al-Duaij, O.; Fawcett, J.; Jones, R. C.; Singh, K. Alkyne insertion into cyclometallated pyrazole and imine complexes of iridium, rhodium and ruthenium; relevance to catalytic formation of carbo- and heterocycles. *Dalton Trans.* **2010**, *39*, 10447-10457. (e) Espada, M. F.; Poveda, M. L.; Carmona, E. Reactivity of a cationic $(C_5Me_5)Ir^{III}$-cyclometalated phosphine complex with alkynes. *Organometallics* **2014**, *33*, 7164−7175. (f) Sun, R.; Zhang, S.; Chu, X.; Zhu, B. Synthesis, structures, and reactivity of cyclometalated complexes formed by insertion of alkynes into M−C (M = Ir and Rh) bonds. *Organometallics* **2017**, *36*, 1133−1141. (g) Giner, E. A.; Gómez-Gallego, M.; Merinero, A. D.; Casarrubios, L.; Ramírez de Arellano, C.; Sierra, M. A. Sequential Reactions of alkynes on an iridium(III) single site. *Chem. Eur. J.* **2017**, *23*, 8941−8948.

(13) Hartwig, J. F. Migratory insertion reactions. In Organotransition Metal Chemistry: From Bonding to Catalysis; University Science Books: USA, 2010; pp 349−396.

(14) We have determined the kinetic order in MeCN, adding 5, 10 and 20 equiv of the stabilizing ligand.

(15) We added excess of MeCN to slow down the formation of the annulated product and observe the conversion of **1-MeCN** into **2a-MeCN**.

(16) Under these reaction conditions, at longer reaction times, we observed a mass balance problem associated to the low solubility of **3a**.

(17) (a) Mendes, P. GEPASI: a software package for modelling the dynamics, steady states and control of biochemical and other systems. *Bioinformatics* **1993**, *9*, 563−571. (b) Mendes, P. Biochemistry by numbers: simulation of biochemical pathways with Gepasi 3. *Trends Biochem. Sci.* **1997**, *22*, 361−363. (c) Mendes, P.; Kell, D. B. Non-linear optimization of biochemical pathways: applications to metabolic engineering and parameter estimation. *Bioinformatics* **1998**, *14*, 869−883. (d) Martins, A. M.; Mendes, P.; Cordeiro, C.; Freire, A. P. In situ kinetic analysis of glyoxalase I and glyoxalase II in Saccharomyces cerevisiae. *Eur. J. Biochem.* **2001**, *268*, 3930−3936.

(18) To enable the full characterization by NMR spectroscopy of **2b-MeCN** and **2c-MeCN**, we added different amounts of MeCN depending on their reactivity. Since **2c-MeCN** turned to be more unstable, instead of 20 equiv, we added 50 equiv.

(19) (a) Otley, K. D.; Ellman, J. A. An efficient method for the preparation of styrene derivatives via Rh(III)-catalyzed direct C−H vinylation. *Org. Lett.* **2015**, *17*, 1332−1335.

(20) Zell, D.; Müller, V.; Dhana, U.; Bursch, M.; Rubio, R.; Grimme, S.; Ackermann, L. Mild cobalt(III)-catalyzed allylative C−F/C−H functionalizations at room temperature. *Chem. Eur. J.* **2017**, *23*, 12145−12148.

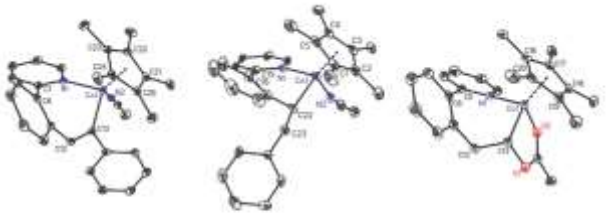

[1,2]-insertion *[1,1]-insertion* *[1,2]-insertion*

This Forum article explores mechanistic details of the migratory insertion step, one of the fundamental steps in organometallic chemistry, in the context of Cp*Co-catalyzed C–H functionalization reactions. Using a direct analogue of a C–H activated Co^{III} metallacycle, we unravel different reactivities and regioselectivities, depending on the stereoelectronic properties of the selected unsaturated molecule.